Provided for non-commercial research and education use.
Not for reproduction, distribution or commercial use.

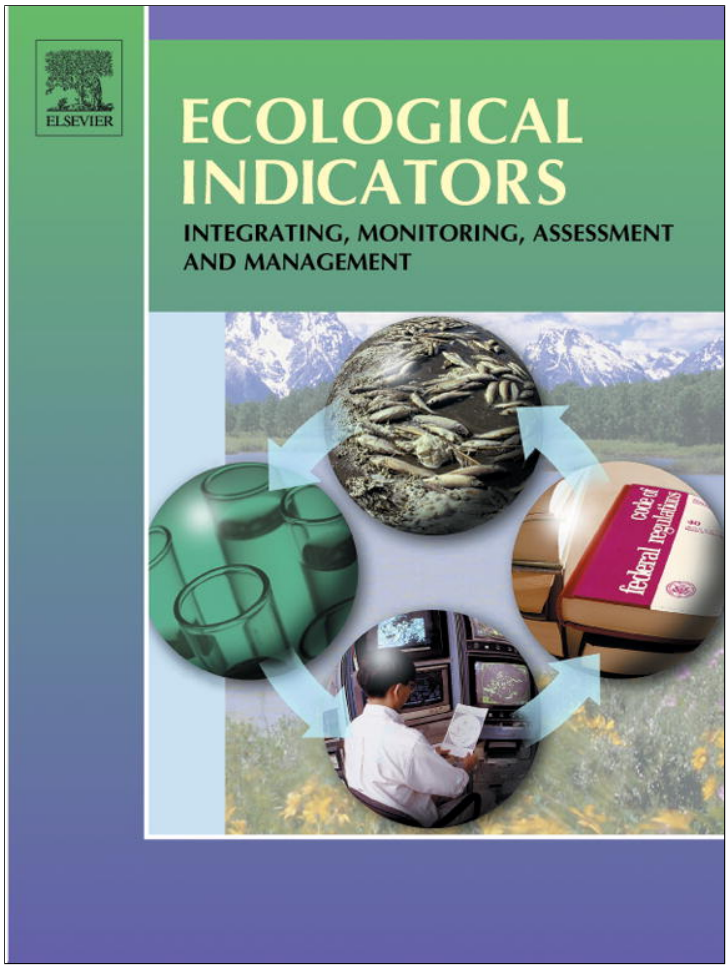

(This is a sample cover image for this issue. The actual cover is not yet available at this time.)

This article appeared in a journal published by Elsevier. The attached copy is furnished to the author for internal non-commercial research and education use, including for instruction at the authors institution and sharing with colleagues.

Other uses, including reproduction and distribution, or selling or licensing copies, or posting to personal, institutional or third party websites are prohibited.

In most cases authors are permitted to post their version of the article (e.g. in Word or Tex form) to their personal website or institutional repository. Authors requiring further information regarding Elsevier's archiving and manuscript policies are encouraged to visit:

http://www.elsevier.com/copyright

Author's personal copy

Ecological Indicators 29 (2013) 203–207

Contents lists available at SciVerse ScienceDirect

Ecological Indicators

journal homepage: www.elsevier.com/locate/ecolind

Short communication

Deriving land surface phenology indicators from CO_2 eddy covariance measurements

Alemu Gonsamo [a,*], Jing M. Chen [a], Petra D'Odorico [b]

[a] Department of Geography and Program in Planning, University of Toronto, Sidney Smith Hall, 100 St. George Street, Room 5047, Toronto, Ontario M5S 3G3, Canada
[b] Remote Sensing Laboratories, University of Zurich - Irchel, Winterhurerstrasse 190, CH-8057 Zurich, Switzerland

ARTICLE INFO

Article history:
Received 28 April 2012
Received in revised form
13 December 2012
Accepted 30 December 2012

Keywords:
Land surface phenology
Remote sensing
GPP
Eddy covariance
Flux
Curve fitting

ABSTRACT

Recent progress of CO_2 eddy covariance (EC) technique and accumulation of measurements offer an unprecedented perspective to study the land surface phenology (LSP) in a more objective way than previously possible by allowing the actual photosynthesis measurement – gross primary productivity (GPP). Because of the spatial, temporal, and ecological complexity of processes controlling GPP time series, the extraction of important LSP dates from GPP has been elusive. Here, we present objective measures of several LSP metrics from GPP time series data. A case study based on long term GPP measurements over a mature boreal deciduous forest is provided together with LSP estimates from remote sensing data. Results show that most LSP metrics are interrelated within each season (spring and autumn) both from GPP and remote sensing based estimates. We provide simple mathematical derivatives of GPP time series to objectively estimate key LSP metrics such as: the start, end and length of growing season; end of greenup; start of browndown; length of canopy closure; start, end and length of peak; and peak of season. These key LSP metrics indicate the collective ecological responses to environmental changes over space and time.

© 2013 Elsevier Ltd. All rights reserved.

1. Introduction

Phenology affects nearly all aspects of ecology and evolution from individual physiology to interspecific relationships to global nutrient fluxes (Forrest and Miller-Rushing, 2010). Recent years have seen a surge of studies vis-à-vis phenological responses and climate change. Land surface phenology (LSP) defined as the study of the timing of recurring seasonal pattern of variation in vegetated land surfaces observed from synoptic sensors (Gonsamo et al., 2012a,b), is a key and a collective indicator of ecosystem dynamics under a changing environment. LSP provides aggregated information at moderate to coarse spatial resolutions, which relate to the timing of vegetation growth, senescence, dormancy, and associated surface phenomena at seasonal and interannual scales. Over the last three decades, numerous studies have used the time series data of vegetation indices derived from land surface reflectance acquired by optical satellite sensors to delineate LSP (e.g., White et al., 2009). Recent progress of CO_2 eddy covariance (EC) technique and accumulation of measurements offer a new perspective for extracting LSP through gross primary productivity (GPP). Increasing number of studies are using GPP measures for key LSP day of year (DOY) extraction (e.g. Ahrends et al., 2009; Gonsamo et al., 2012a,b; Gu et al., 2009; Noormets et al., 2009; Richardson et al., 2010; Wu and Chen, 2013) due to its compatible spatial footprint with coarse and medium resolution satellite pixels and objective land surface measure of photosynthesis (Chen et al., 2010; Gonsamo et al., 2012a). Despite large progress in LSP metrics extraction from remote sensing observations, the key LSP DOYs are often extracted arbitrarily from EC based measures of GPP. For example, Richardson et al. (2010) discussed the use of various methods to extract start of growing season (SOS) and end of growing season (EOG) from GPP measures: the first and last DOY at which specific absolute thresholds of daily GPP reached 2, 4 or 6 g C m-2 d-1; and the first and last DOY at which relative thresholds (defined in terms of maximum GPP, the peak value of daily GPP) of daily GPP reached 25%, 50% and 75% of maximum GPP. Because of the spatial, temporal, and ecological complexity of GPP variations, the functional relevance of any particular threshold can be elusive and thus the use of arbitrary thresholds to define SOS and EOS becomes problematic. Gu et al. (2009) and Noormets et al. (2009) discussed the use of logistic regressions for LSP DOYs retrievals, but without analytical solutions to extract various LSP metrics. Here we present objective approaches to extract several important LSP metrics from EC based GPP measures. This short communication also compares the LSP dates extracted from GPP with that of improved remote sensing based retrievals.

* Corresponding author. Tel.: +1 416 946 7715; fax: +1 416 946 3886.
E-mail addresses: gonsamoa@geog.utoronto.ca, ggalex2002@yahoo.com (A. Gonsamo).

1470-160X/$ – see front matter © 2013 Elsevier Ltd. All rights reserved.
http://dx.doi.org/10.1016/j.ecolind.2012.12.026

Author's personal copy

Table 1
Formula for the computation of the LSP metrics from eddy covariance GPP time series.

Fig. 1 label (derivatives)	LSP metrics	Formulae from Eq. (1) parameters
b (1st)	Mid of greenup (MOG)	β_1
h (1st)	Mid of browndown (MOB)	β_2
a (3rd)	Start of season (SOS)	$\beta_1 - (4.562/2\partial_1)$
i (3rd)	End of season (EOS)	$\beta_2 + (4.562/2\partial_2)$
i (3rd) - a (3rd)	Length of season (LOS)	$\beta_2 + (4.562/2\partial_2) - \beta_1 + (4.562/2\partial_1)$
c (2nd)	End of greenup (EOG)	$\beta_1 + (1.317/\partial_1)$
g (2nd)	Start of browndown (SOB)	$\beta_2 - (1.317/\partial_2)$
g (2nd) - c (2nd)	Length of canopy closure (LOCC)	$\beta_2 - (1.317/\partial_2) - \beta_1 - (1.317/\partial_1)$
d (3rd)	Start of peak (SOP)	$\beta_1 + (4.562/2\partial_1)$
f (3rd)	End of peak (EOP)	$\beta_2 - (4.562/2\partial_2)$
f (3rd) - d (3rd)	Length of peak (LOP)	$\beta_2 - (4.562/2\partial_2) - \beta_1 - (4.562/2\partial_1)$
e (2nd)	Peak of season (POS)	$-1.317(-\partial_1 - \beta_1)$

2. LSP metrics from GPP measurements

The annual cycle of LSP inferred from GPP is characterized by several key transition dates, which define the key phenological phases of vegetation dynamics at annual time scales (Table 1 and Fig. 1). These transition dates include key LSP dates such as: the start of growing season (SOS), end of growing season (EOS), length of growing season (LOS), end of greenup (EOG), start of browndown (SOB), length of canopy closure (LOCC), start of peak (SOP), end of peak (EOP), length of peak (LOP), and peak of season (POS). These LSP metrics indicate the collective ecological responses to environmental changes over space and time and some have previously been used in remote sensing based LSP studies (e.g., Ahl et al., 2006; Busetto et al., 2010; Noormets et al., 2009; Zhang et al., 2003). Here, we present a new method, which fits EC GPP measures to a logistic function of time. Based on this function, the transition dates defined above can be identified in a systematic fashion. At regional and larger scales, variations in community composition, micro- and regional climate regimes, soils, and land management result in complex spatio-temporal variation in LSP. Therefore, the LSP determination from the GPP measures should allow flexibility to represent the variability in vegetation temporal dynamics. The temporal variation in GPP data for an entire growing cycle can be modeled using a function of the form:

$$f(x) = \alpha_1 + \frac{\alpha_2}{1 + e^{-\partial_1(x-\beta_1)}} - \frac{\alpha_3}{1 + e^{-\partial_2(x-\beta_2)}} \quad (1)$$

where $f(x)$ is the observed GPP at day of year (DOY) x, α_1 is the background GPP, $\alpha_2 - \alpha_1$ is the difference between the background and the amplitude of the spring and early summer plateau, and $\alpha_3 - \alpha_1$ is the difference between the background and the amplitude of the late summer and autumn plateau both in GPP units. ∂_1 and ∂_2 are the transitions curvature parameters (normalized slope coefficients), and β_1 and β_2 are the midpoints in DOYs of these transitions for greenup and browndown, respectively. The first, second and third derivatives of $\hat{y}$ of Eq. (1) are given by:

$$f'(x) = \frac{\alpha_2 \partial_1 e^{\partial_1(x+\beta_1)}}{\left(e^{\partial_1\beta_1} + e^{\partial_1 x}\right)^2} - \frac{\alpha_3 \partial_2 e^{\partial_2(x+\beta_2)}}{\left(e^{\partial_2\beta_2} + e^{\partial_2 x}\right)^2} \quad (2)$$

$$f''(x) = \frac{\alpha_2 \partial_1^2 (e^{\partial_1(x+2\beta_1)} - e^{\partial_1(2x+\beta_1)})}{\left(e^{\partial_1\beta_1} + e^{\partial_1 x}\right)^3} + \frac{\alpha_3 \partial_2^2 e^{\partial_2(x+\beta_2)}(e^{\partial_2 x} - e^{\partial_2\beta_2})}{\left(e^{\partial_2\beta_2} + e^{\partial_2 x}\right)^3} \quad (3)$$

$$f'''(x) = \frac{\alpha_2 \partial_1^3 (-4e^{2\partial_1(x+\beta_1)} + e^{\partial_1(x+3\beta_1)} + e^{\partial_1(3x+\beta_1)})}{\left(e^{\partial_1\beta_1} + e^{\partial_1 x}\right)^4} - \frac{\alpha_3 \partial_2^3 (-4e^{2\partial_2(x+\beta_2)} + e^{\partial_2(3\beta_2+x)} + e^{\partial_2(\beta_2+3x)})}{\left(e^{\partial_2\beta_2} + e^{\partial_2 x}\right)^4} \quad (4)$$

For each site-year, the seven parameters describing the shape of the fitting curve can be determined by least squares

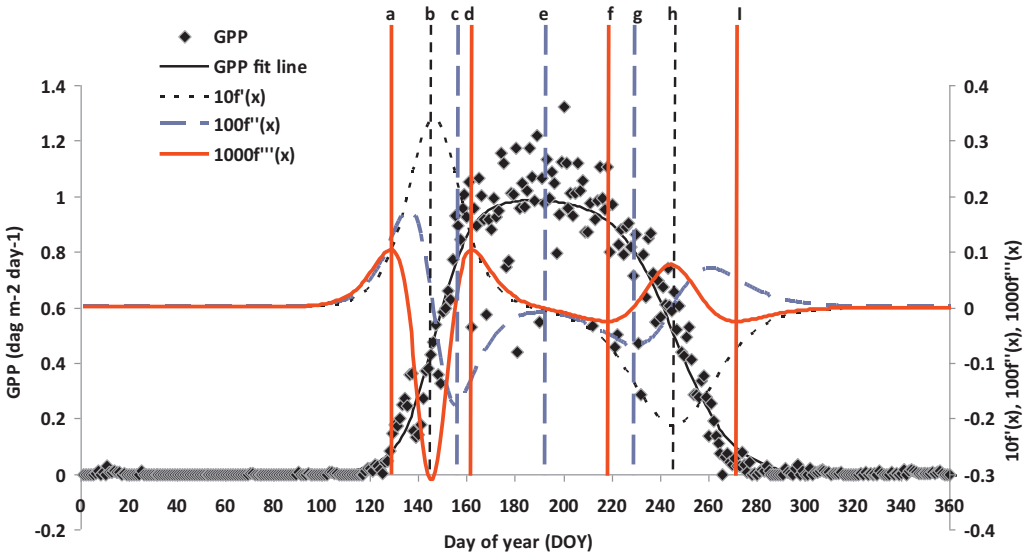

Fig. 1. Seasonal course of gross primary productivity (GPP), and the land surface phenology metrics (denoted with letters, *a–i*) as defined by the extremes of the first ($f'(x)$), second ($f''(x)$), and third ($f'''(x)$) derivatives of the fitted logistic function Eq. (1). The scales of the derivatives are enhanced for visual clarity. The GPP measures are from the Canadian old Aspen flux tower site for year 2007. dag = dekagram.

Author's personal copy

minimization of the differences between Eq. (1) and the GPP time series. The DOYs at which the fitted logistic curve showed characteristic curvature changes (LSP metrics) were identified with the formula shown in Table 1 derived analytically from the seven parameters of Eq. (1) corresponding to the minimums and maximums of the derivatives (Eqs. (2)–(4)). Several LSP metrics were identified in both the spring and autumn seasons (Table 1 and Fig. 1). Metrics $\beta_1(\beta_2)$ are the dates of maximum increase (decrease) of the fitted curve, which are frequently used to estimate the start and end of the growing season dates from remote sensing data (White et al., 2009). Given the DOYs of the midpoints of spring greenup (β_1) and autumn browndown (β_2), the spring plateau (α_2) and ranges in GPP ($\alpha_2 - \alpha_1$), the autumn plateau (α_3) and ranges in GPP ($\alpha_3 - \alpha_1$), and the average slopes of the spring ($\alpha_2\partial_1/4.562$) and the autumn ($\alpha_3\partial_2/4.562$) linear transition lines (Ricketts and Head, 1999), we can estimate the minimums and maximums of the third derivatives analytically by applying triangle identity theory. Mathematically, the upper ends of the linear part of the greenup curve can be expressed as $\beta_1 + (1.317/\partial_1)$ whereas the browndown curve is $\beta_2 - (1.317/\partial_2)$, both corresponding to the second derivative (Eq. (3)) (details for derivation of inflection points from sigmoid curves can be found in statistical books, e.g. Johnson et al., 1974). The use of seven-parameter logistic function (Eq. (1)) instead of the traditional six-parameter function (e.g. Fisher et al., 2006) gives robust statistical confidence for analytical solutions by allowing the use of different amplitudes during the spring and autumn halves of the growing seasons with the intention that the ascendant (greenup) and descendent (browndown) parts can differ both in shape and in maximum values. The analytical formula to derive all LSP metrics using the GPP measurements are given in Table 1. These formula apply to all unimodal GPP curves and avoid the complicated analysis of derivates to retrieve phenologically important dates.

Metrics SOS, EOP and SOP, EOS are the dates defined by the intersect of the tangent at the steepest part of the curves and of the tangents at the asymptotic starts and asymptotic ends of the curves, respectively corresponding to the roots of the third derivative of the fitted curve (Eq. (4), Table 1 and Fig. 1). Thus, the length of the growing season (LOS) and peak (LOP) can be calculated from the differences between EOS and SOS and EOP and SOP, respectively. Metrics EOG (SOB) correspond to the threshold of the end of greenup (start of browndown) and are obtained from the minimums of the second derivatives (Eq. (3), Table 1 and Fig. 1) corresponding to the end and start of linear part of the curve in spring and autumn seasons, respectively. We define the time between EOG and SOB as the length of canopy closure (LOCC) indicating the period between the onset and offset of maximum leaf area index for a given environmental and edaphic condition of the site in a given year. In the same manner, the threshold date between the greenup and browndown can be obtained from the maximum of the second derivatives between EOG and SOB corresponding to the peak DOY of the growing season (POG) (Eq. (3), Table 1 and Fig. 1).

3. Case study on long term GPP measurements over mature deciduous forest site

3.1. Site description

We used CO_2 flux data from a deciduous forest site of the Canadian Carbon Program (CCP) network, formerly known as FLUXNET-Canada to demonstrate the phenology metrics determinations. The Saskatchewan Old Aspen (OA) flux site represents the only broadleaf forest flux tower site over Canada, importantly located in a transitional zone between boreal forest and grassland (lat: 53.62889/lon: −106.19779). The forest site representing the largest dominant and co-dominant overstorey broadleaf tree species over the North American boreal zone is characterized by a mean air temperature of 0.4 °C and a mean annual precipitation of ~467 mm (Barr et al., 2004; Bergeron et al., 2007). The aspen trees at this site are on average 21 m tall and 90 year old with a few Balsam Poplar and thick Hazel understory with total leaf area index of 2.1 (Chen et al., 2006).

3.2. GPP measurements

We used 15 site-years of GPP data available from the CCP website (http://www.fluxnet-canada.ca/) measured using the EC technique for the years 1996—2010. Wind velocity components (u, v, w, measured using 3-D sonic anemometers), air temperature, water vapor density, and CO_2 concentration were sampled at 10 to 20 Hz, and calculations of relevant covariances were performed from these samples to obtain the fluxes. A standard procedure was used to estimate the daily GPP from half-hourly values of net ecosystem exchange (NEE) (Barr et al., 2004). NEE was calculated as the sum of the EC CO_2 flux above the canopy and the change in CO_2 storage in the air column between the EC-sensor height and the ground. Net ecosystem productivity (NEP) was calculated as NEP = − NEE. Measured ecosystem respiration (Re) was estimated as Re = − NEP during periods when GPP was known to be zero, i.e., at night and during both night and day in the cold season (periods when both air and soil temperatures are less than 0 °C). Data gaps due to instrument malfunction, power failure, and calibration schedule were filled using linear interpolation and relationships between Re and NEE and various climatic and biological variables (Barr et al., 2004). Finally, GPP (dekagram m-2 d-1) was calculated as the sum of NEP and Re:

$$\mathrm{GPP} = \mathrm{NEP} + \mathrm{Re} \tag{5}$$

Daily GPP data were fitted to the logistic function with a nonlinear regression provided with the first guess values of the seven parameters in Eq. (1), and solved with maximum of 2000 iterations. All of the LSP metrics were derived from the seven parameters of Eq. (1) as described in Table 1.

3.3. MODIS 500 m reflectance data

We used the MODIS surface reflectance product, MOD09A1 to compare the SOS and EOS DOYs derived from GPP to that of remote sensing observations. In the production of MOD09A1, atmospheric corrections for gases, thin cirrus clouds and aerosols are implemented (Vermote and Vermeulen, 1999). The MOD09A1 product is produced in 8-day 'maximum quality' composites in 500 m pixels, choosing observations with minimal cloud cover, low solar zenith angles, and near-nadir views. The selected MOD09A1 surface reflectance product consisted of ASCII subsets for the CO_2 flux tower site from the DAAC database at the Oak Ridge National Laboratory (http://daac.ornl.gov/MODIS/). We have extracted the red, near infrared (NIR), and shortwave infrared (SWIR) reflectances and the exact acquisition date for a single 500 m pixel at the tower site for the period spanning from February 2000 to December 31st 2010, intersecting all available MODIS time series with GPP measurements. Ninety percent of stable (day time) CO_2 flux, used for GPP, usually comes from the area less than 500 m of the tower site (Chen et al., 2009).

We have used the newly developed phenology index (PI: Gonsamo et al., 2012a,b) to derive remote sensing based SOS and EOS dates from MODIS data. The PI is calculated as follows:

$$\mathrm{PI} = \begin{cases} 0, \text{ if NDVI or NDII} < 0 \\ \mathrm{NDVI}^2 - \mathrm{NDII}^2 \\ 0, \text{ if PI} < 0 \end{cases} \tag{6}$$

Author's personal copy

where NDVI is the normalized difference vegetation index (NDVI = (NIR − red)/(NIR + red)) and NDII is the normalized difference infrared index (NDII = (NIR − SWIR)/(NIR + SWIR)). The SOS and EOS dates derived from PI using Eq. (1) were proven to be better phenology estimates compared to NDVI (Gonsamo et al., 2012a,b). Both SOS and EOS were derived after fitting Eq. (1) in the same manner as GPP, i.e. SOS = $\beta_1 - (4.562/2\partial_1)$ whereas EOS = $\beta_2 + (4.562/2\partial_2)$ corresponding to the same phenology metrics from GPP (Table 1). A simple weighting scheme was used to filter out the noisy data, which gives a weight of half for the sum-of-squared-error for the value of PI of the central point if they are less than half or more than twice of the median value of the moving window of three points in the iterative curve fitting process.

3.4. Results

Fig. 2 presents the LSP metrics derived from EC based GPP measurements (*a*–*i*) and remote sensing data (SOS and EOS). The study by Gonsamo et al. (2012a) demonstrated the strong agreement between the SOS and EOS DOYs derived from EC GPP and remote sensing PI with average error of less than 8 days. PI also follows the land surface photosynthesis (GPP) better than other commonly used vegetation indices (Gonsamo et al., 2012a). The current study further shows that the SOS derived from GPP explains 85% (R^2 = 0.85) variability of SOS from PI whereas only 50% (R^2 = 0.5) variability is explained in the case of EOS (i.e., GPP SOS = *a*, and GPP EOS = *i*: Fig. 2). The explained variance of EOS is less than SOS due to difficulty in estimating the slow process of vegetation browning and leaf abscission. The results show that the use of a more objective approach such as the logistic function used here is feasible for LSP metrics retrievals from EC GPP measures. The interannual variabilities of the spring LSP metrics (i.e., *a*–*d* and SOS) and the autumn LSP metrics (i.e., *f*–*i* and EOS) follow the same patter within each season (Fig. 2).

The SOS came early for years 1998, 2001, 2006 and 2010 because the average air temperature of April and May were the highest for these four years. Start of peak (SOP = *d*) and peak of season (POS = *e*) came late for year 2004 because the average temperature of May and June were the lowest for this year. For year 2003, the autumn LSP metrics such as the start of browndown (SOB) and end of peak (EOP) came earlier due to the record high temperature of July and August for this year compared to other years although the end of season (EOS) was comparable with other years (Fig. 2). Fig. 2 also shows that the greenup is faster than the browndown. A close examinations of Fig. 1 and GPP time series from other years indicate that the commonly accepted use of subjective GPP thresholds (e.g., Richardson et al., 2010) such as 2, 4 or 6 g C m-2 d-1, or 25%, 50% and 75% of maximum GPP in both spring and autumn seasons overestimate SOS and underestimate EOS compared to remote sensing LSP dates. In spring season, the 25% of maximum GPP lies halfway between lines *a* and *b*, 50% equals line *b*, and 75% lies halfway between lines *b* and *d* whereas, in autumn season the 25% of maximum GPP lies halfway between lines *h* and *i*, 50% equals line *h*, and 75% lies halfway between lines *f* and *h* (Figs. 1 and 2). In spring season, both 50% and 75% threshold of maximum GPP overestimate SOS compared to remote sensing estimates whereas 25% gives reasonably close estimate to SOS (Fig. 2). The same is true for threshold using the absolute values where 4 and 6 g C m-2 d-1 overestimate the SOS and 2 g C m-2 d-1 gives comparable results with remote sensing based estimates of SOS. In autumn season, all of the six percent and absolute value thresholds (e.g., Richardson et al., 2010: such as 2, 4 or 6 g C m-2 d-1, or 25%, 50% and 75% of maximum GPP) underestimate EOS compared to the remote sensing based EOS estimates (Fig. 2).

Gu et al. (2003) and Noormets et al. (2009) used a Weibull function which treats two parts of a growing season separately, creating a discontinuity both in the fit lines and derivatives, with conditional assumptions of separation. They use subjective and visual approaches to extract LSP metrics. Gu et al. (2009) later used a seven parameter logistic function to fit GPP time series, but they failed to derive important LSP metrics analytically. Our function (Eq. (1)) is continues, derivable, flexible, and easy to extract LSP metrics analytically from first estimates of the seven parameters without complex derivative analysis. Ahrends et al. (2009) presented visual evaluation of phenology metrics from webcam and GPP time series, but without LSP metrics from GPP. Gonsamo et al. (2012a) provides detailed comparison of GPP and PI time series and SOS and EOS metrics from the two datasets. They however do not provide the remaining LSP metrics given in Table 1, which are required to study the LSP time series throughout the year. The LSP metrics in Table 1 are collective indictors of the interactions between the

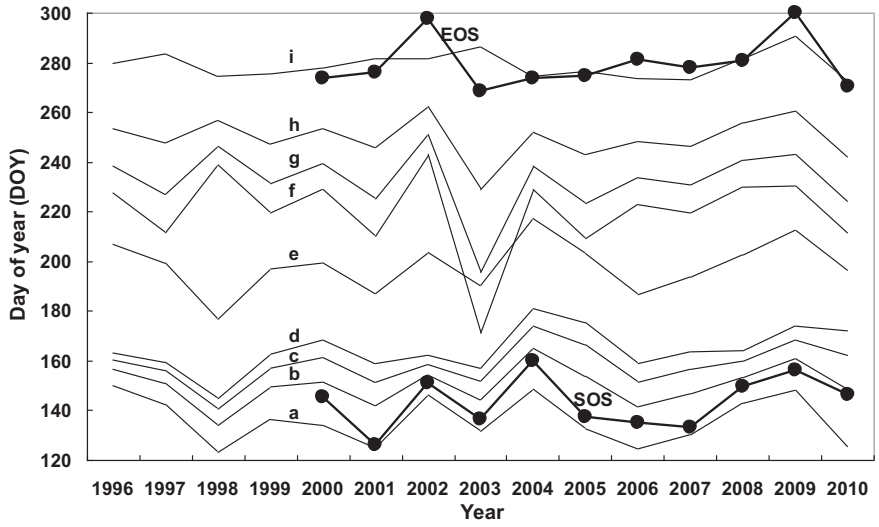

Fig. 2. Seasonal course of the land surface phenology metrics (denoted with letters, *a*–*i*, Table 1) as defined by the extremes of the first, second, and third derivatives of the fitted double logistic function Eq. (1) to gross primary productivity (GPP). Start of season (SOS) and end of season (EOS) derived from the remote sensing phenology index (PI) are also plotted for years 2000–2010.

Author's personal copy

inherent biological and ecological processes and the progression of climatic conditions and reflects unique functioning of plant communities at different stages of the growing season. Besides the key LSP DOYs, we can also retrieve analytically the rate parameters. For example, from Eq. (1), average slopes of the spring (average recovery rate indicating the average greenup rate) and the autumn (average senescence rate indicating the average browndown rate) can be retrieved as $\alpha_2\partial_1/4.562$ and $\alpha_3\partial_2/4.562$, respectively. The peak recovery rate in spring and senescence rate in autumn are ∂_1 and ∂_2, respectively. These LSP metrics and rates provide us tools to develop a unique photosynthetic signature for each plant community. These coupled with mechanistic explanations of the underlying processes will help develop new ecological theories and in-depth physiological and biochemical studies. PI and the GPP based LSP metrics need further studies, particularly in moisture limited ecosystem with tropical, subtropical, and Mediterranean vegetation sites. For multimodal GPP curves as those of managed crop lands with two or more growing periods within a year, Eq. (1) should be applied for each bell curves separately. Further study should also look into detailed uncertainty analysis with representative study sites from global distributions of plant functional types and biomes.

4. Conclusions

Land surface phenology (LSP) has seen a surge of interest due to its collective response to climatic controls over terrestrial ecosystem. Previous studies have often focused on the use of remote sensing data for retrieving LSP metrics (White et al., 2009). However, a survey of late 20th and early 21st century LSP literature for North America highlights the conflicting results of SOS and EOS obtained from satellite based methods, due in large part to the problems associated with LSP methodologies. One objective way of estimating LSP is by direct measurement of land surface photosynthesis using EC techniques. However, the use of subjective thresholds to extract important LSP dates from EC GPP has been elusive. In this study, we have provided objective measures to retrieve several LSP metrics from EC GPP measurements. These metrics not only help the detailed study of the climatic control over LSP, but also provide validation data to compare the remote sensing based LSP estimates.

Acknowledgments

This study is supported by an NSERC Strategic Grant (STPGP 381474-09). We thank the FLUXNET-Canada (Canadian Carbon Program) network, the site principal investigators, co-investigators, participants, and data collection and processing staff for contributing to the tower flux data, and the agencies and institutions that funded long-term measurements at these sites. We thank the MODIS land product processing team at Oak Ridge National Laboratory Distributed Active Archive Center (ORNL DAAC) for the MODIS Collection 5 data. We would like to thank two anonymous referees for extremely helpful comments.

Appendix A. Supplementary data

Supplementary data associated with this article can be found, in the online version, at http://dx.doi.org/10.1016/j.ecolind.2012.12.026. These data include Google maps of the most important areas described in this article.

References

Ahl, D.E., Gower, S.T., Burrows, S.N., Shabanov, N.V., Myneni, R.B., Knyazikhin, Y., 2006. Monitoring spring canopy phenology of a deciduous broadleaf forest using MODIS. Remote Sens. Environ. 104, 88–95.

Ahrends, H.E., Etzold, S., Kutsch, W.L., Stoeckli, R., Bruegger, R., Jeanneret, F., Wanner, H., Buchmann, N., Eugster, W., 2009. Tree phenology and carbon dioxide fluxes: use of digital photography at for process-based interpretation the ecosystem scale. Clim. Res. 39, 261–274.

Barr, A.G., Black, T.A., Hogg, E.H., Kljun, N., Morgenstern, K., Nesic, Z., 2004. Inter-annual variability in the leaf area index of a boreal aspen-hazelnut forest in relation to net ecosystem production. Agr. Forest Meteorol. 126, 237–255.

Bergeron, O., Margolis, H.A., Black, T.A., Coursolle, C., Dunn, A.L., Barr, A.G., Wofsy, S.C., 2007. Comparison of carbon dioxide fluxes over three boreal black spruce forests in Canada. Glob. Change Biol. 13, 89–107.

Busetto, L., Colombo, R., Migliavacca, M., Cremonese, E., Meroni, M., Galvagno, M., Rossini, M., Siniscalco, C., Morra Di Cella, U., Pari, E., 2010. Remote sensing of larch phenological cycle and analysis of relationships with climate in the Alpine region. Glob. Change Biol. 16, 2504–2517.

Chen, B., Black, T.A., Coops, N.C., Hilker, T., Trofymow, J.A., Morgenstern, K., 2009. Assessing tower flux footprint climatology and scaling between remotely sensed and eddy covariance measurements. Bound. Layer Meteorol 130, 137–167.

Chen, B., Coops, N.C., Fu, D., Margolis, H.A., Amiro, B.D., Barr, A.G., Black, T.A., Arain, M.A., Bourque, C.P.-A., Flanagan, L.B., Lafleur, P.M., McCaughey, J.H., Wofsy, S.C., 2010. Assessing eddy-covariance flux tower location bias across the Fluxnet-Canada Research Network based on remote sensing and footprint modeling. Agric. Forest Meteorol. 151, 87–100.

Chen, J.M., Govind, A., Sonnentag, O., Zhang, Y., Barr, A., Amiro, B., 2006. Leaf area index measurements at Fluxnet-Canada forest sites. Agr. Forest Meteorol. 140, 257–268.

Fisher, J.I., Mustard, J.F., Vadeboncoeur, M.A., 2006. Green leaf phenology at Landsat resolution: scaling from the field to the satellite. Remote Sens. Environ. 100, 265–279.

Forrest, J., Miller-Rushing, A.J., 2010. Toward a synthetic understanding of the role of phenology in ecology and evolution. Philos. Trans. R. Soc. Lond. 365, 3101–3112.

Gonsamo, A., Chen, J.M., Price, D.T., Kurz, W.A., Wu, C., 2012a. Land surface phenology from optical satellite measurement and CO_2 eddy covariance technique. J. Geophys. Res. 117, G03032.

Gonsamo, A., Chen, J.M., Wu, C., Dragoni, D., 2012b. Predicting deciduous forest carbon uptake phenology by upscaling FLUXNET measurements using remote sensing data. Agric. Forest Meteorol. 165, 127–135.

Gu, L., Post, W.M., Baldocchi, D.D., Black, T.A., Suyker, A.E., Verma, S.B., Vesala, T., Wofsy, S.C., 2009. Characterizing the seasonal dynamics of plant community photosynthesis. In: Noormets, A. (Ed.), Phenology of Ecosystem Processes: Applications in Global Change Research. Springer, New York.

Gu, L., Post, W.M., Baldocchi, D., Black, T.A., Verma, S.B., Vesala, T., Wofsy, S.C., 2003. Phenology of vegetation photosynthesis. In: Schwartz, M.D. (Ed.), Phenology: an Integrated Environmental Science. Kluwer, Dordecht.

Johnson, F.H., Eyring, H., Stover, B.J., 1974. The Theory of Rate Processes in Biology and Medicine. John Wiley & Sons, New York.

Noormets, A., Chen, J., Gu, L., Desai, A., 2009. The phenology of gross ecosystem productivity and ecosystem respiration in temperate hardwood and conifer chronosequences. In: Noormets, A. (Ed.), Phenology of Ecosystem Processes: Applications in Global Change Research. Springer, New York.

Richardson, A.D., Black, T.A., Ciais, P., Delbart, N., Friedl, M.A., Gobron, N., Hollinger, D.Y., Kutsch, W.L., Longdoz, B., Luyssaert, S., Migliavacca, M., Montagnani, L., Munger, J.W., Moors, E., Piao, S.L., Rebmann, C., Reichstein, M., Saigusa, N., Tomelleri, E., Vargas, R., Varlagin, A., 2010. Influence of spring and autumn phenological transitions on forest ecosystem productivity. Philos. Trans. R. Soc. B. 365 (1555), 3227–3246.

Ricketts, J.H., Head, G.A., 1999. A five parameter logistic equation for investigating asymmetry of curvature in baroreflex studies. Am. J. Physiol.: Regul. Integr. Comp. Physiol. 277, R441–R454.

Vermote, E.F., Vermeulen, A., 1999. Atmospheric Correction Algorithm: Spectral Reflectances (MOD09), Algorithm Technical Background Document available online at http://modis.gsfc.nasa.gov/data/atbd/atbd_mod08.pdf

White, M.A., de Beurs, K.M., Didan, K., Inouye, D.W., Richardson, A.D., Jensen, O.P., O'Keefe, J., Zhang, G., Nemani, R.R., van Leeuwen, W.J.D., Brown, J.F., de Wit, A., Schaepman, M., Lin, X., Dettinger, M., Bailey, A.S., Kimball, J., Schwartz, M.D., Baldocchi, D.D., Lee, J.T., Lauenroth, W.K., 2009. Intercomparison, interpretation, and assessment of spring phenology in North America estimated from remote sensing for 1982–2006. Glob. Change Biol. 15, 2335–2359.

Wu, C., Chen, J.M., 2013. Deriving a new phenological indicator of interannual net carbon exchange in contrasting boreal deciduous and evergreen forests. Ecol. Indic. 24, 113–119.

Zhang, X.Y., Friedl, M.A., Schaaf, C.B., Strahler, A.H., Hodges, J.C.F., Gao, F., Reed, B.C., Huete, H., 2003. Monitoring vegetation phenology using MODIS. Remote Sens. Environ. 84, 471–475.